# Square-Wave Voltammetry

Valentin Mirčeski
Šebojka Komorsky-Lovrić
Milivoj Lovrić

# Square-Wave Voltammetry

## Theory and Application

Springer

Šebojka Komorsky-Lovrić
Ruder Bošković Institute
Center for Marine
and Environmental Research
P.O. Box 180
10002 Zagreb
Croatia
*slovric@rudjer.irb.hr*

Milivoj Lovrić
Ruder Bošković Institute
Center for Marine
and Environmental Research
Bijenicka 54
10002 Zagreb
Croatia
*slovric@rudjer.irb.hr*

Valentin Mirčeski
Institute of Chemistry
Faculty of Natural Sciences and Mathematics
"Ss Cyril and Methodius" University
PO Box 162
1000 Skopje
Republic of Macedonia
*valentin@iunona.pmf.ukim.edu.mk*

ISBN-13: 978-3-540-73739-1 e-ISBN-13: 978-3-540-73740-7

Library of Congress Control Number: 2007931853



Cover design: WMX Design GmbH, Heidelberg
Typesetting and Production: LE-TEX Jelonek, Schmidt & Vöckler GbR, Leipzig

Printed on acid-free paper

9 8 7 6 5 4 3 2 1

springer.com

# Preface

This is the first monograph in a series devoted to electrochemistry. Although the market is rich in books and series on electrochemical themes, it is surprising that a number of serious topics are not available. With the series "Monographs in Electrochemistry" an attempt will be made to fill these gaps. I am very thankful to the publishing house of Springer for agreeing to publish these books, and for the great freedom given to me in choosing the topics and the most competent authors, and generally for the fantastic cooperation with the publisher. I am especially thankful to Mr. Peter W. Enders.

Square-wave voltammetry is a technique that is readily available to anyone applying modern electrochemical measuring systems. Its use can be beneficial in analytical applications as well as in fundamental studies of electrode mechanisms. Upon first glance, it seems that the analytical application of square-wave voltammetry is rather simple and does not afford a deep knowledge of the background, however, this is certainly not the case. For an optimal exploitation of the potential of square-wave voltammetry, it is essential to know how the signal is generated and how its properties depend on the kinetics and thermodynamics of the electrode processes. For a detailed analysis of electrode mechanisms, this is indispensable, of course, in any case. I am very happy that three leading experts in the field of square-wave voltammetry have agreed to write the present monograph, which in fact is the first complete book on that technique ever published in English. All three authors have a long and distinguished publishing record in electroanalysis, and especially in the theory and application of square-wave voltammetry. I hope that this monograph will make it much easier for potential users in research, industrial, and environmental laboratories, etc., to apply square-wave voltammetry for their benefit.

Fritz Scholz
– *Editor of the series* "*Monographs in Electrochemistry*" –

# Contents

# Chapter 1
# Introduction

## 1.1 From Square-Wave Polarography to Modern Square-Wave Voltammetry

Square-wave voltammetry (SWV) is a powerful electrochemical technique that can be applied in both electrokinetic and analytic measurements [1–5]. The technique originates from the Kalousek commutator [6] and Barker's square-wave polarography [7]. Kalousek constructed an instrument with a rotating commutator that switched the potential of the dropping mercury electrode between two voltage levels with the frequency of five cycles per second [8, 9]. Three methods for programming the voltages have been devised and designated as types I, II, and III, and these are shown in Fig. 1.1. Type I polarograms were recorded by superimposing a low-amplitude square-wave (20 – 50 mV peak-to-peak) onto the ramp voltage of conventional polarography. The current was recorded during the higher potential half-cycles only. Figure 1.2 shows the theoretical response of a simple and electrochemically reversible electrode reaction:

$$\mathrm{O}^{m+} + n\,\mathrm{e}^- \leftrightarrows \mathrm{R}^{(m-n)+} \tag{1.1}$$

obtained by the type I program. Only the reactant $\mathrm{O}^{m+}$ is initially present in the bulk of the solution. The starting potential is $-0.25$ V vs. $E_{1/2}$, where $E_{1/2}$ is a half-wave potential of dc polarogram of electrode reaction (1.1). The response is characterized by a maximum oxidation current appearing at 0.034 V vs. $E_{1/2}$. In the vicinity of the half-wave potential, the reactant is reduced during the lower potential half-cycle (which is not recorded) and the product is oxidized during the higher potential half-cycle, which is recorded. This is illustrated in Fig. 1.3, which shows theoretical concentrations of the reactant and product near the electrode surface at the end of the last cathodic (A) and anodic (B) half-cycles applied to the same drop. The method was improved by Ishibashi and Fujinaga, who introduced the differential polarography by measuring the difference in current between successive half-cycles of the square-wave signal [10–12]. The frequency of the signal was 14 Hz. It was superimposed on a rapidly changing potential ramp and applied to the single mercury

V. Mirčeski, Š. Komorsky-Lovrić, M. Lovrić, *Square-Wave Voltammetry*
doi: 10.1007/978-3-540-73740-7, 

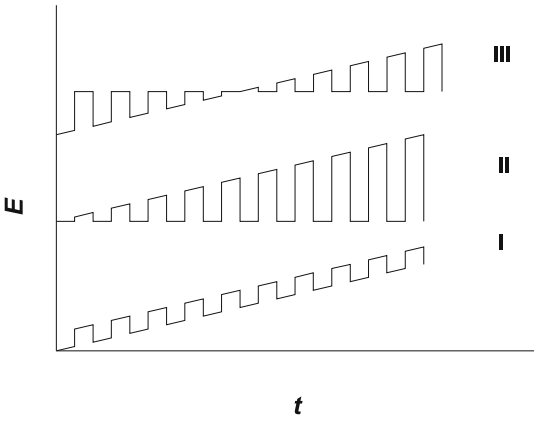


**Fig. 1.1** Potential-time relationships realized by the Kalousek commutator

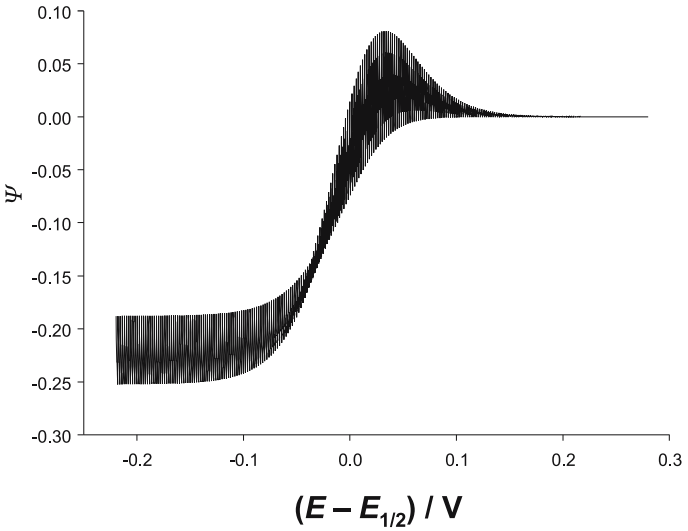


**Fig. 1.2** Type I Kalousek polarogram of electrode reaction (1.1) on dropping mercury electrode. $\Psi = I/nFA_m c_O^* (Df)^{1/2}$, frequency = 5 Hz, amplitude = 30 mV, drop life time = 1 s, $\mathrm{d}E/\mathrm{d}t$ = 2 mV/s and $E_{st} = -0.25$ V vs. $E_{1/2}$. For the meaning of symbols, see below (1.9) and (1.24)

drop. Barker and Jenkins introduced three important innovations: (i) the frequency of square-wave signal was 225 Hz, (ii) the current was measured during the last 280 µs of each half-cycle and the difference between two successive readings was recorded, and (iii) the measurement was performed only once in the life of each drop 250 ms before its end [13, 14]. Figure 1.5 shows the theoretical square-wave polarogram of the electrode reaction (1.1) under the same conditions as in Fig. 1.2. The response is a bell-shaped current-voltage curve with its maximum at −0.016 V vs. $E_{1/2}$. Each current-voltage step corresponds to a separate mercury drop. The objec-

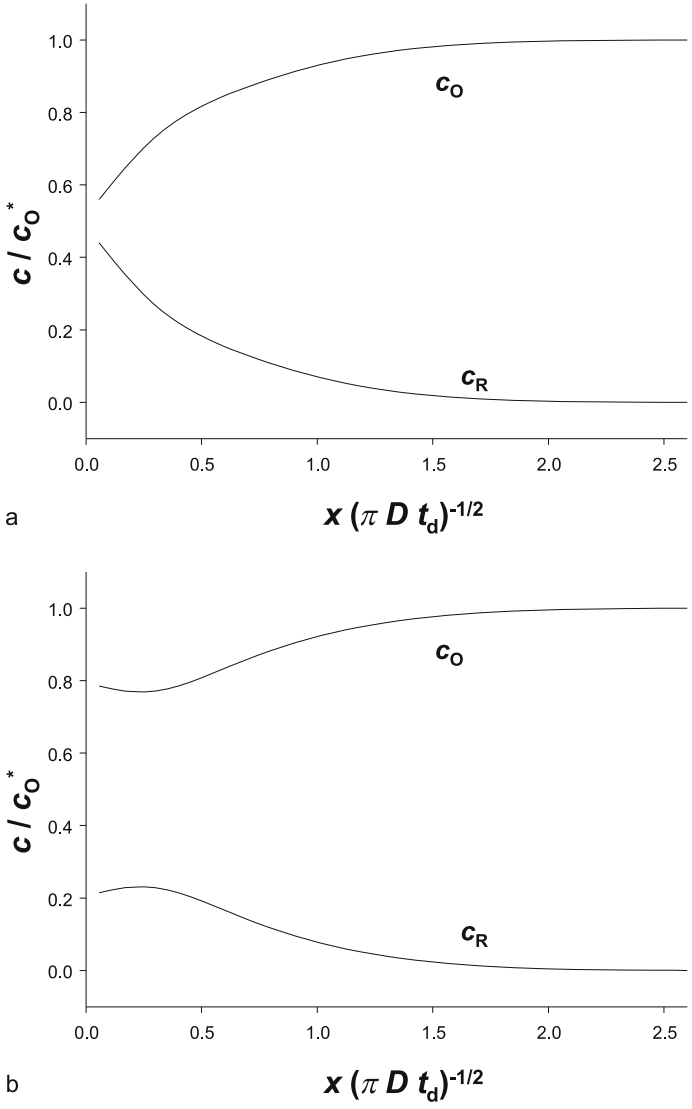


**Fig. 1.3** Concentrations of the reactant and product of the electrode reaction (1.1) near the electrode surface at the end of the last cathodic (**a**) and anodic (**b**) Kalousek type I half-cycles applied to the same drop. $E = 0.004$ (**a**) and 0.034 V vs. $E_{1/2}$ (**b**). All other data are as in Fig. 1.2

tive of Barker's innovations was to minimize the influence of capacity current, i.e., to discriminate that current with respect to the faradaic current. During each half-cycle, the double layer charging current decreases exponentially with time, while the faradaic current is inversely proportional to the square-root of time. Under certain conditions, the charging current at the end of half-cycle may be smaller than the faradaic current. A theoretical example is shown in Fig. 1.6. Generally, the charg-

**Fig. 1.4** Portraits of Mirko Kalousek (*left*) and Geoffrey Barker (*right*) (reprinted from [66] and [67] with permission)

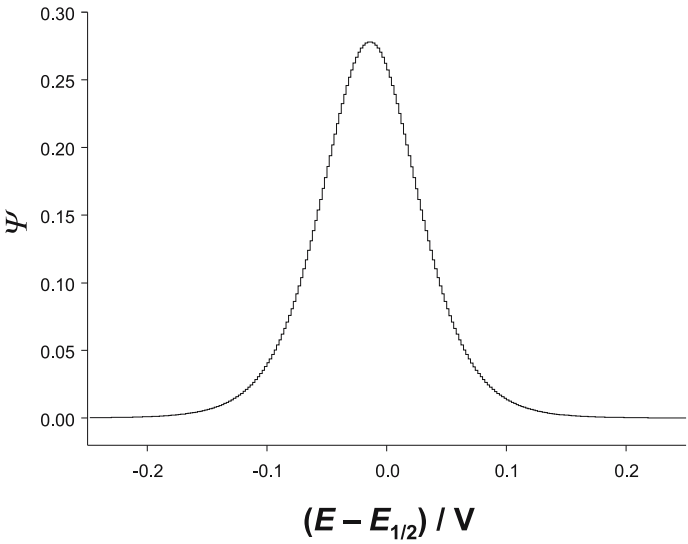


**Fig. 1.5** Barker square-wave polarogram of electrode reaction (1.1) on dropping mercury electrode. $\Psi = I/nFA_m c_O^* (Df)^{1/2}$, frequency = 225 Hz, amplitude = 30 mV, drop life time = 1 s, $dE/dt = 2\,\mathrm{mV/s}$ and $E_{st} = -0.25$ V vs. $E_{1/2}$

ing current is partly eliminated by the subtraction of currents measured at the end of two successive half-cycles. This is because the charging current depends on the difference between the electrode potential and its potential of zero charge. If the square-wave amplitude is small, the difference between the charging currents of the cathodic and anodic half-cycles is also small, and for this reason, square-wave

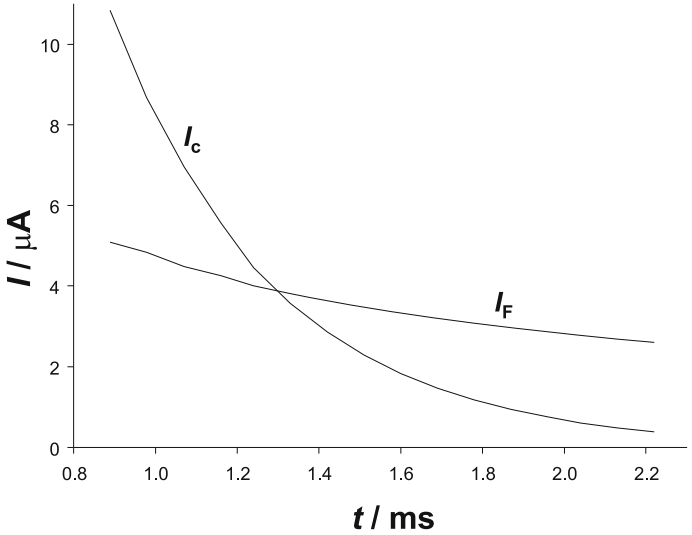


**Fig. 1.6** A scheme of a double layer charging current ($I_C$) and the Faradaic current ($I_F$) during the second half of the last half-cycle of square-wave signal applied to the dropping mercury electrode. $E - E_{1/2} = -0.016$ V, $E - E_{pzc} = 0.1$ V, $C = 40\,\mu F/cm^2$, $R = 10\,\Omega$, $A_m = 0.01\,cm^2$, $D = 9 \times 10^{-6}\,cm^2/s$, $n = 1$, $c_O^* = 5 \times 10^{-4}$ mol/L and $f = 225$ Hz

voltammetry and differential pulse polarography and voltammetry are discriminating against a capacitive current [1, 3, 15–19].

This method was developed further by superimposing the square-wave signal onto a staircase signal [20, 21]. Some of the possible potential-time waveforms are shown in Fig. 1.7. Usually, each square-wave cycle occurs during one stair-

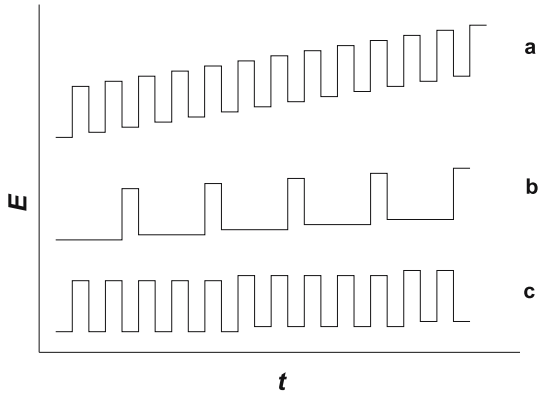


**Fig. 1.7** Potential-time waveforms obtained by superimposing the square-wave signal onto a staircase signal: square-wave voltammetry (*a*), differential pulse voltammetry (*b*) and multiple square-wave voltammetry (*c*)

case period, which is sometimes called Osteryoung SWV [20–23], but in multiple square-wave voltammetry, several cycles are applied on the single tread [24,25]. The asymmetric signal (b) in Fig. 1.7 is a general form of differential pulse voltammetry [22,23]. These complex excitation signals were applied to stationary electrodes, or a single mercury drop. More details can be found in several reviews [26–40].

## 1.2 Square-Wave Voltammetry: Calculations and Instrumentation

Figure 1.8 shows the potential-time waveform of the modern SWV [41]. Comparing to curve (a) in Fig. 1.7, the starting potential is a median of extreme potentials of the square-wave signal. To each tread of the staircase signal a single square-wave cycle is superimposed, so the waveform can be considered as a train of pulses towards higher and lower potentials added to the potential that changes in a stepwise manner. The magnitude of each pulse, $E_{sw}$, is one-half of the peak-to-peak amplitude of the square-wave signal. For historical reasons, the pulse height $E_{sw}$ is called the square-wave amplitude [1]. The duration of each pulse is one-half the staircase period: $t_p = \tau/2$. The frequency of the signal is the reciprocal of the staircase period: $f = 1/\tau$. The potential increment $\Delta E$ is the height of the staircase waveform. Relative to the scan direction, $\Delta E$, forward and backward pulses can be distinguished. The currents are measured during the last few microseconds of each pulse and the difference between the current measured on two successive pulses of the same step

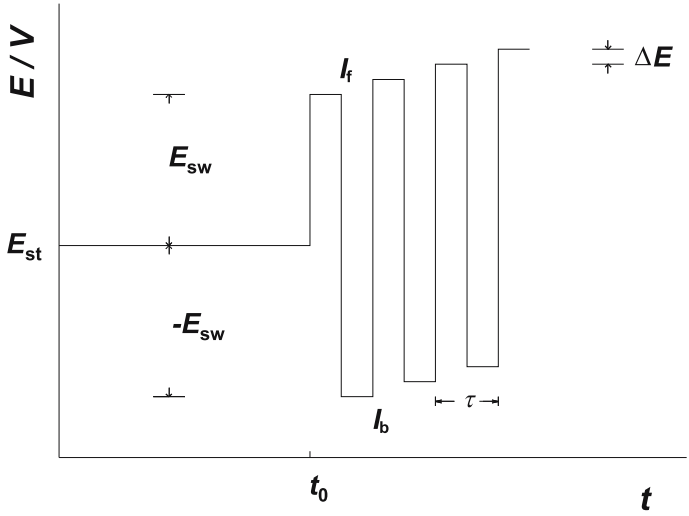


**Fig. 1.8** Scheme of the square-wave voltammetric excitation signal. $E_{st}$ starting potential, $E_{sw}$ pulse height, $\Delta E$ potential increment, $\tau$ staircase period, $t_0$ delay time and $I_f$ and $I_b$ denote the points where the forward and backward currents are sampled, respectively

is recorded as a net response ($\Delta I = I_f - I_b$). For analytical purposes, several instantaneous currents can be sampled at certain intervals during the last third, or some other portion of the pulse, and then averaged. This is done because the response appears less noisy if the sampling window is wider [42,43]. The two components of the net response, $I_f$ and $I_b$, i.e., the currents of the forward and the backward series of pulses, respectively, are also displayed. The currents are plotted as a function of the corresponding potential of the staircase waveform. The delay period, $t_0$, which may precede the signal, is used for the accumulation of the reactant on the working electrode surface in order to record the stripping process.

SWV experiments are usually performed on stationary solid electrodes or static mercury drop electrodes. The response consists of discrete current-potential points separated by the potential increment $\Delta E$ [1, 20–23]. Hence, $\Delta E$ determines the apparent scan rate, which is defined as $\Delta E/\tau$, and the density of information in the response, which is a number of current-potential points within a certain potential range. The currents increase proportionally to the apparent scan rate. For better graphical presentation, the points can be interconnected, but the line between two points has no physical significance, as there is no theoretical reason to interpolate any mathematical function between two experimentally determined current-potential points. The currents measured with smaller $\Delta E$ are smaller than the values predicted by the interpolation between two points measured with bigger $\Delta E$ [3]. Frequently, the response is distorted by electronic noise and a smoothing procedure is necessary for its correct interpretation. In this case, it is better if $\Delta E$ is as small as possible. By smoothing, the set of discrete points is transformed into a continuous current-potential curve. Care should be taken that the smoothing procedure does not distort the square-wave response.

A solution of the diffusion equation for an electrode reaction for repetitive stepwise changes in potential can be obtained by numerical integration [44]. For a stationary planar diffusion model of a simple, fast, and reversible electrode reaction (1.1), the following differential equations and boundary conditions can be formulated:

$$\partial c_O/\partial t = D(\partial^2 c_O/\partial x^2) \tag{1.2}$$

$$\partial c_R/\partial t = D(\partial^2 c_R/\partial x^2) \tag{1.3}$$

Initially, only the reactant $O^{m+}$ is present in the solution and its concentration is uniform:

$$t = 0: \quad c_O = c_O^* \, , \, c_R = 0 \tag{1.4}$$

At the infinite distance from the electrode surface, the concentrations of the reactant and product do not change:

$$t > 0 \, , \, x \to \infty: \quad c_O \to c_O^* \, , \, c_R \to 0 \tag{1.5}$$

The current is proportional to the gradient of concentration of product at the electrode surface:

$$x = 0: \quad D(\partial c_O/\partial x)_{x=0} = -I/nFA \tag{1.6}$$

$$D(\partial c_R/\partial x)_{x=0} = I/nFA \tag{1.7}$$

The concentrations of reactant and product at the electrode surface are connected by the Nernst equation:

$$(c_O)_{x=0} = (c_R)_{x=0} \exp(\varphi) \tag{1.8}$$

$$\varphi = (nF/RT)(E - E^\theta) \tag{1.9}$$

Here $c_O$ and $c_R$ are the concentrations of the reactant and product, respectively, $D$ is a common diffusion coefficient, $c_O^*$ is the bulk concentration of the reactant, $I$ is the current, $n$ is the number of electrons, $F$ is the Faraday constant, $A$ is the electrode surface area, $E$ is electrode potential, $E^\theta$ is the standard potential, $R$ is the gas constant, $T$ is absolute temperature, $x$ is the distance from the electrode surface and $t$ is the time variable [45].

Using the Laplace transformations of the reactant concentration and its derivative on time [46]:

$$\mathscr{L}c_O = \int_0^\infty c_O \exp(-st)\,\mathrm{d}t \tag{1.10}$$

$$\mathscr{L}(\partial c_O/\partial t) = s\mathscr{L}c_O - (c_O)_{t=0} \tag{1.11}$$

the differential equation (1.2) can be transformed into:

$$\partial^2 u/\partial x^2 - (s/D)\,u = 0 \tag{1.12}$$

where $u = \mathscr{L}c_O - c_O^*/s$ and $s$ is the transformation variable. The boundary conditions are:

$$x \to \infty: \quad u \to 0 \tag{1.13}$$

$$x = 0: \quad (\partial u/\partial x)_{x=0} = -\mathscr{L}I/nFAD \tag{1.14}$$

The general solution of (1.12) is:

$$u_{1,2} = K_1 \exp(-(s/D)^{1/2}x) + K_2 \exp((s/D)^{1/2}x) \tag{1.15}$$

A particular solution is obtained by using (1.13) and (1.14):

$$K_2 = 0 \tag{1.16}$$

$$K_1 = s^{-1/2}\mathscr{L}I/nFAD^{1/2} \tag{1.17}$$

$$(\mathscr{L}c_O)_{x=0} = c_O^*/s + s^{-1/2}\mathscr{L}I/nFAD^{1/2} \tag{1.18}$$

By the inverse Laplace transformation of (1.18) an integral equation is obtained [46]:

$$(c_{\mathrm{O}})_{x=0} = c_{\mathrm{O}}^{*} + (nFA)^{-1}(D\pi)^{-1/2} \int_{0}^{t} I(\tau)(t-\tau)^{-1/2}\,\mathrm{d}\tau \tag{1.19}$$

Within each time interval from 0 to $t$, the current $I$ depends on the variable $\tau$. The integral $\int f(\tau)g(t-\tau)\,\mathrm{d}\tau$ is called the convolution of functions $f$ and $g$.

The solution of (1.3) is obtained by the same procedure:

$$(c_{\mathrm{R}})_{x=0} = -(nFA)^{-1}(D\pi)^{-1/2} \int_{0}^{t} I(\tau)(t-\tau)^{-1/2}\,\mathrm{d}\tau \tag{1.20}$$

The convolution integral in (1.19) and (1.20) can be solved by the method of numerical integration proposed by Nicholson and Olmstead [47]. The time $t$ is divided into $m$ time increments: $t = md$. It is assumed that within each time increment the function $I$ can be replaced by the average value $I_j$:

$$\int_{0}^{t} I(\tau)(t-\tau)^{-1/2}\,\mathrm{d}\tau = \sum_{j=1}^{m} I_j \int_{(j-1)d}^{jd} (md-\tau)^{-1/2}\,\mathrm{d}\tau \tag{1.21}$$

The integral in (1.21) is solved by the substitution $p = md - \tau$:

$$\int_{(j-1)d}^{jd} (md-\tau)^{-1/2}\,\mathrm{d}\tau = 2d^{1/2}[(m-j+1)^{1/2} - (m-j)^{1/2}] \tag{1.22}$$

Each square-wave half-period is divided into 25 time increments: $d = (50f)^{-1}$. By introducing (1.19) and (1.20) into (1.8), the following system of recursive formulae is obtained:

$$\Psi_1 = -5(\pi/2)^{1/2}(1+\exp(\varphi_1))^{-1} \tag{1.23}$$

$$\Psi_m = -5(\pi/2)^{1/2}(1+\exp(\varphi_m))^{-1} - \sum_{j=1}^{m-1} \Psi_j S_{m-j+1} \tag{1.24}$$

where $\Psi = I/nFAc_{\mathrm{O}}^{*}(Df)^{1/2}$, $S_1 = 1$, $S_k = k^{1/2} - (k-1)^{1/2}$, $\varphi_m = (nF/RT)(E_m - E^{\theta})$, $m = 2, 3, \ldots M$ and $M = -50\,(E_{\mathrm{fin}} - E_{\mathrm{st}})/\Delta E$. The potential $E_m$ changes according to Fig. 1.8.

If the electrode reaction (1.1) is kinetically controlled, (1.8) must be substituted by the Butler–Volmer equation:

$$I/nFA = -k_{\mathrm{s}}\exp(-\alpha\varphi)[(c_{\mathrm{O}})_{x=0} - (c_{\mathrm{R}})_{x=0}\exp(\varphi)] \tag{1.25}$$

where $k_s$ is the standard rate constant and $\alpha$ is the cathodic transfer coefficient. In this case, the following recursive formulae are obtained [44, 48–50]:

$$\Psi_1 = -\frac{\kappa \exp(-\alpha\varphi_1)}{1+\kappa\exp(-\alpha\varphi_1)\frac{\sqrt{2}}{5\sqrt{\pi}}[1+\exp(\varphi_1)]} \tag{1.26}$$

$$\Psi_m = -Z_1 - Z_2 \sum_{j=1}^{m-1} \Psi_j S_{m-j+1} \tag{1.27}$$

$$Z_1 = \frac{\kappa \exp(-\alpha\varphi_m)}{1+\kappa\exp(-\alpha\varphi_m)\frac{\sqrt{2}}{5\sqrt{\pi}}[1+\exp(\varphi_m)]} \tag{1.28}$$

$$Z_2 = \frac{\kappa \exp(-\alpha\varphi_m)\frac{\sqrt{2}}{5\sqrt{\pi}}[1+\exp(\varphi_m)]}{1+\kappa\exp(-\alpha\varphi_m)\frac{\sqrt{2}}{5\sqrt{\pi}}[1+\exp(\varphi_m)]} \tag{1.29}$$

where $\kappa = k_s(Df)^{-1/2}$ is a dimensionless kinetic parameter and the meanings of other symbols are given below (1.24).

The developments of instrumentation for Kalousek [31, 51, 52] and square-wave polarography [53–58] and square-wave voltammetry [59–65] are mainly of historical interest. Today, many computer-controlled potentiostats/galvanostats providing SWV signal generation are available from numerous manufacturers, such as Eco-Chemie (models PGSTAT 10, 12, 20, 30, 100 and 302 and μAutolab I, II, and III), Metrohm (models VA 646 and 797 Computrace), Princeton Applied Research (models 263A, 273A, 283, 2263, 2273, and 384B), Bioanalytical Systems (models 100A, 100B/W and Epsilon), Cypress Systems (models CS 1090 and 1200 and CYSY-2), Amel Srl (models 433, 7050 and 7060), Gamry Instruments (models PCI 4/300 and 4/750), Analytical Instrument Systems (models LCP-200 and DLK-100), Uniscan Instruments (model PG 580), Palm Instruments (model Palmsens), Rudolph Instruments (model GATTEA 4000 AS) and IVA Company (model IVA-5).

# References


1. Osteryoung J, O'Dea JJ (1986) Square-wave voltammetry. In: Bard AJ (ed) Electroanalytical chemistry, vol 14. Marcel Dekker, New York, p 209
2. Eccles GN (1991) Crit Rev Anal Chem 22:345
3. Lovrić M (2002) Square-wave voltammetry. In: Scholz F (ed) Electroanalytical methods, Springer, Berlin Heidelberg New York, p 111
4. de Souza D, Machado SAS, Avaca LA (2003) Quim Nova 26:81
5. de Souza D, Codognoto L, Malagutti AR, Toledo RA, Pedrosa VA, Oliveira RTS, Mazo LH, Avaca LA, Machado SAS (2004) Quim Nova 27:790
6. Ružić I (1972) J Electroanal Chem 39:111
7. Barker GC, Gardner AW (1992) Analyst 117:1811
8. Kalousek M (1946) Chem Listy 40:149
9. Kalousek M (1948) Coll Czechoslov Chem Commun 13:105
10. Ishibashi M, Fujinaga T (1950) Bull Chem Soc Jpn 23:261
11. Ishibashi M, Fujinaga T (1952) Bull Chem Soc Jpn 25:68
12. Ishibashi M, Fujinaga T (1952) Bull Chem Soc Jpn 25:238
13. Barker GC, Jenkins IL (1952) Analyst 77:685
14. Barker GC (1958) Anal Chim Acta 18:118
15. Turner JA, Christie JH, Vuković M, Osteryoung RA (1977) Anal Chem 49:1904
16. Barker GC, Gardner AW (1979) J Electroanal Chem 100:641
17. Stefani S, Seeber R (1983) Ann Chim 73:611
18. Dimitrov JD (1997) Anal Lab 6:87
19. Dimitrov JD (1998) Anal Lab 7:3
20. Ramaley L, Krause MS Jr (1969) Anal Chem 41:1362
21. Krause MS Jr, Ramaley L (1969) Anal Chem 41:1365
22. Rifkin SC, Evans DH (1976) Anal Chem 48:1616
23. Christie JH, Turner JA, Osteryoung RA (1977) Anal Chem 49:1899
24. Fatouros N, Simonin JP, Chevalet J, Reeves RM (1986) J Electroanal Chem 213:1
25. Krulic D, Fatouros N, Chevalet J (1990) J Electroanal Chem 287:215
26. Milner GWC, Slee LJ (1957) Analyst 82:139
27. Hamm RE (1958) Anal Chem 30:351
28. Saito Y, Okamoto K (1962) Rev Polarog 10:227
29. Kaplan BY, Sorokovskaya II (1962) Zavod Lab 28:1053
30. Geerinck G, Hilderson H, Vanttulle C, Verbeck F (1963) J Electroanal Chem 5:48
31. Kinard WF, Philp RH, Propst RC (1967) Anal Chem 39:1556
32. Geissler M, Kuhnhardt C (1970) Square-wave polarographie. VEB Deutscher Verlag für Grundstoffindustrie, Leipzig
33. Kaplan BY, Sevastyanova TN (1971) Zh Anal Khim 26:1054
34. Igolinskii VA, Kotova NA (1973) Elektrokhimiya 9:1878

35. Sturrock PE, Carter RJ (1975) Crit Rev Anal Chem 5:201
36. Blutstein H, Bond AM (1976) Anal Chem 48:248
37. Kopanica M, Stara V (1981) J Electroanal Chem 127:255
38. Alexander PW, Akapongkul V (1984) Anal Chim Acta 166:119
39. Ramaley L, Tan WT (1981) Can J Chem 59:3326
40. Hwang JY, Wang YY, Wan CC (1986) J Chin Chem Soc 33:303
41. Osteryoung JG, Osteryoung RA (1985) Anal Chem 57:101 A
42. Aoki K, Maeda K, Osteryoung J (1989) J Electroanal Chem 272:17
43. Zachowski EJ, Wojciechowski M, Osteryoung J (1986) Anal Chim Acta 183:47
44. O'Dea JJ, Osteryoung J, Osteryoung RA (1981) Anal Chem 53:695
45. Galus Z (1994) Fundamentals of electrochemical analysis. Ellis Horwood, New York, Polish Scientific Publishers PWN, Warsaw
46. Spiegel MR (1965) Theory and problems of Laplace transforms. McGraw-Hill, New York
47. Nicholson RS, Olmstead ML (1972) Numerical solutions of integral equations. In: Matson JS, Mark HB, MacDonald HC (eds) Electrochemistry: calculations, simulations and instrumentation, vol 2. Marcel Dekker, New York, p 119
48. O'Dea JJ, Osteryoung J, Osteryoung RA (1983) J Phys Chem 87:3911
49. O'Dea JJ, Osteryoung J, Lane T (1986) J Phys Chem 90:2761
50. Nuwer MJ, O'Dea JJ, Osteryoung J (1991) Anal Chim Acta 251:13
51. Radej J, Ružić I, Konrad D, Branica M (1973) J Electroanal Chem 46:261
52. Paspaleev E, Batsalova K, Kunchev K (1979) Zavod Lab 45:504
53. Ferrett DJ, Milner GWC, Shalgosky HI, Slee LJ (1956) Analyst 81:506
54. Taylor JH (1964) J Electroanal Chem 7:206
55. Buchanan EB, McCarten JB (1965) Anal Chem 37:29
56. Kalvoda R, Holub I (1973) Chem Listy 67:302
57. Barker GC, Gardner AW, Williams MJ (1973) J Electroanal Chem 42:App 21
58. Buchanan EB Jr, Sheleski WJ (1980) Talanta 27:955
59. Yarnitzky C, Osteryoung RA, Osteryoung J (1980) Anal Chem 52:1174
60. He P, Avery JP, Faulkner LR (1982) Anal Chem 54:1313 A
61. Anderson JE, Bond AM (1983) Anal Chem 55:1934
62. Lavy-Feder A, Yarnitzky C (1984) Anal Chem 56:678
63. Jayaweera P, Ramaley L (1986) Anal Instrum 15:259
64. Poojary A, Rajagopalan SR (1986) Indian J Technol 24:501
65. Wong KH, Osteryoung RA (1987) Electrochim Acta 32:629
66. Bard AJ, Inzelt G, Scholz F (2007) Electrochemical dictionary. Springer, Berlin Heidelberg New York
67. Parsons R (1977) J Electroanal Chem 75:1

# Chapter 2
# Electrode Mechanisms

## 2.1 Electrode Reactions of Dissolved Species on Stationary Planar Electrodes

### *2.1.1 Reversible Electrode Reactions*

Figure 2.1 shows computed square-wave voltammogram of the simple, fast and electrochemically reversible electrode reaction (1.1), i.e., $O^{m+} + n\,e^- \leftrightarrows R^{(m-n)+}$. The response was calculated by using (1.23) and (1.24). The dimensionless net response ($\Delta\Psi = -\Delta I/nFAc_O^*(Df)^{1/2}$), where $\Delta I = I_f - I_b$, and its forward (reductive) ($\Psi_f$), and backward (oxidative) ($\Psi_b$) components are shown. The meanings of other symbols are given below (1.9). The voltammogram is characterized by the maximum net response, which is also called the net peak current, $\Delta I_p$. The corresponding staircase potential is the net peak potential $E_p$. Other characteristics are the minimum of the reductive component, the maximum of the oxidative component and their potentials. The net peak potential and the peak potentials of both components are independent of SW frequency. This is one of various indications that the electrode reaction is electrochemically reversible within the range of applied frequencies [1–6].

Both the dimensionless net peak current $\Delta\Psi_p$ and the peak width at half-height, or the half-peak width, $\Delta E_{p/2}$ depend on the products "the number of electrons times the SW amplitude", i.e., $nE_{sw}$, and "the number of electrons times the potential increment", i.e., $n\Delta E$. This is shown in Table 2.1 and Fig. 2.2 (curve 1), for the constant product $n\Delta E$. With increasing $nE_{sw}$ the slope $\partial\Delta\Psi_p/\partial nE_{sw}$ continuously decreases, while the gradient $\partial\Delta E_{p/2}/\partial nE_{sw}$ increases. The maximum ratio $\Delta\Psi_p/\Delta E_{p/2}$ appears for $nE_{sw} = 50\,mV$, as can be seen in Fig. 2.2. This is the optimum SW amplitude for analytical measurement [7]. At higher amplitudes the resolution of two peaks is diminished. The ratio of peak currents of the forward and backward components, and the peak potentials of the components are also listed in Table 2.1. If $nE_{sw} > 10\,mV$, the backward component indicates the reversibility of the electrode reaction, and if $nE_{sw} > 5\,mV$, the net peak potential $E_p$ is equal to the half-wave potential of the reversible reaction (1.1). If $E_{sw} = 0$, the square-wave sig-

V. Mirčeski, Š. Komorsky-Lovrić, M. Lovrić, *Square-Wave Voltammetry*
doi: 10.1007/978-3-540-73740-7, 

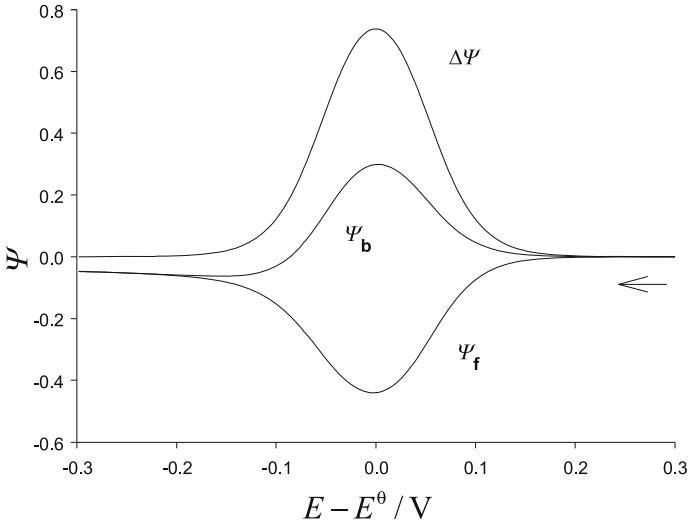


**Fig. 2.1** Theoretical square-wave voltammogram of fast and reversible electrode reaction (1.1). $E_{sw} = 50$ mV, $n = 1$, $E_{st} - E^{\theta} = 0.3$ V, $t_0 = 0$ s and $\Delta E = -2$ mV. The dimensionless net response ($\Delta\Psi$) and its forward ($\Psi_f$) and backward ($\Psi_b$) components

**Table 2.1** Square-wave voltammetry of fast and reversible electrode reaction (1.1). The dimensionless net peak current, the ratio of peak currents of the forward and backward components, the peak potentials of the components and the half-peak width as functions of SW amplitude; $n\Delta E = -2$ mV

| $nE_{sw}$/mV | $\Delta\Psi_p$ | $I_{p,f}/I_{p,b}$ | $E_{p,f} - E_p$/mV | $E_{p,b} - E_p$/mV | $\Delta E_{p/2}$/mV |
|---|---|---|---|---|---|
| 10 | 0.1961 | −10.35 | −12 | 26 | 92 |
| 20 | 0.3701 | −2.78 | −8 | 10 | 96 |
| 30 | 0.5206 | −1.94 | −6 | 6 | 104 |
| 40 | 0.6432 | −1.63 | −4 | 4 | 112 |
| 50 | 0.7383 | −1.47 | −2 | 2 | 124 |
| 60 | 0.8093 | −1.37 | −2 | 2 | 139 |
| 70 | 0.8608 | −1.31 | 0 | 0 | 152 |
| 80 | 0.8975 | −1.27 | 2 | −2 | 168 |
| 90 | 0.9231 | −1.23 | 4 | −2 | 186 |
| 100 | 0.9409 | −1.21 | 6 | −4 | 204 |

nal turns into the signal of differential staircase voltammetry [8–10], and $\Delta\Psi_p$ does not vanish [4]. To establish an additional criterion of the reversibility of the reaction (1.1), the standard SW amplitudes $E_{sw} = 50$, 25 and 15 mV, for $n = 1$, 2 and 3, respectively, and the common potential increment $\Delta E = -2$ mV are proposed. The characteristic data of responses of simple and electrochemically reversible electrode reactions under standard conditions are listed in Table 2.2.

The net peak current depends linearly on the square root of the frequency [5, 11]:

$$\Delta I_p = -nFAD^{1/2}\Delta\Psi_p f^{1/2} c_O^* \tag{2.1}$$

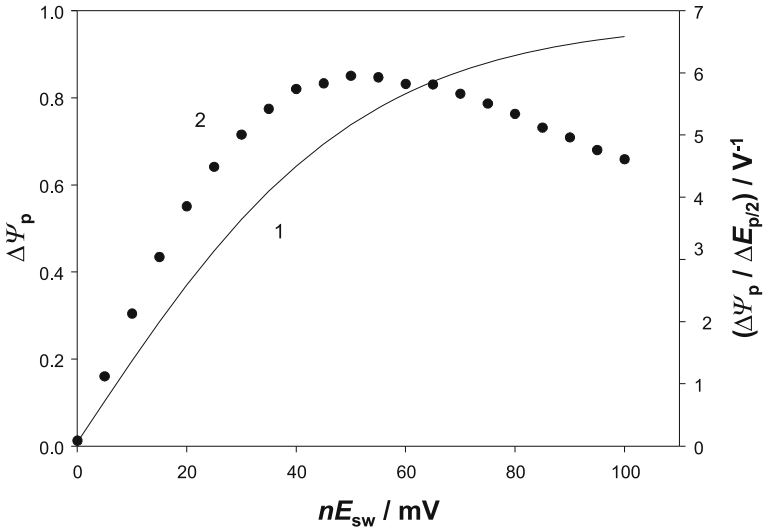


**Fig. 2.2** The dependence of the dimensionless net peak current (*1*) and the ratio of the dimensionless net peak current and the half-peak width (*2*) on the product of number of electrons and the square-wave amplitude

**Table 2.2** Criteria of the reversibility of reaction (1.1). Properties of the response under standard conditions

| $n$ | $\Delta E$/mV | $E_{sw}$/mV | $I_{p,f}/I_{p,b}$ | $E_{p,f} - E_p$/V | $E_{p,b} - E_p$/V | $\Delta E_{p/2}$/mV |
|---|---|---|---|---|---|---|
| 1 | −2 | 50 | −1.47 | −0.002 | 0.002 | 124 |
| 2 | −2 | 25 | −1.70 | −0.002 | 0.002 | 62 |
| 3 | −2 | 15 | −2.03 | −0.002 | 0.002 | 40 |

The condition is that the instantaneous current is sampled during the last few microseconds of the pulse [2, 3]. This procedure was assumed in the theoretical calculations presented in Figs. 2.1 and 2.2, and Tables 2.1 and 2.2. Usually, the current is sampled during a certain portion of the pulse and then averaged. The average response corresponds to an instantaneous current sampled in the middle of the sampling window. For $nE_{sw} = 25$ mV and $n\Delta E = -5$ mV, this relationship is [12]:

$$\Delta I_p = -nFAD^{1/2}c_O^* \, 0.477 t_s^{-1/2}(1 - 0.317\beta^{1/2}) \tag{2.2}$$

where $t_s$ is the sampling time and $\beta = t_s/t_p$ is the pulse fraction at which the current is sampled (see Fig. 2.3). If $\beta$ is constant, the relationship between $\Delta I_p$ and the square-root of the time variable is linear, regardless of whether the frequency, or the reciprocal of sampling time is used as the characteristic variable. This condition is satisfied if the relative size of the sampling window $(s/t_p)$ is constant, because $\beta = 1 - s/2t_p$. If the absolute size of the sampling window is constant (e.g., $s = 1$ ms), its